Noise temperature and beam pattern of an NbN hot electron bolometer mixer at 5.25 THz

W. Zhang, P. Khosropanah, J. R. Gao, T. Bansal, T. M. Klapwijk, W. Miao, and S. C. Shi

Citation: Journal of Applied Physics **108**, 093102 (2010); doi: 10.1063/1.3503279
View online: http://dx.doi.org/10.1063/1.3503279
View Table of Contents: http://scitation.aip.org/content/aip/journal/jap/108/9?ver=pdfcov
Published by the AIP Publishing

Noise temperature and beam pattern of an NbN hot electron bolometer mixer at 5.25 THz

W. Zhang,[1,2,a)] P. Khosropanah,[1] J. R. Gao,[1,3,b)] T. Bansal,[1,3] T. M. Klapwijk,[3] W. Miao,[2] and S. C. Shi[2]
[1]*SRON Netherlands Institute for Space Research, Landleven 12, 9747 AD Groningen, The Netherlands*
[2]*Purple Mountain Observatory, National Astronomical Observatories of China, Chinese Academy of Sciences, 2 West Beijing Road, Nanjing, Jiangsu 210008, China*
[3]*Kavli Institute of Nanoscience, Delft University of Technology, Lorentzweg 1, 2628 CJ Delft, The Netherlands*

(Received 14 April 2010; accepted 16 September 2010; published online 1 November 2010)

We report the measured sensitivities of a superconducting NbN hot electron bolometer (HEB) heterodyne receiver at 5.25 THz. Terahertz (THz) radiation is quasioptically coupled to a HEB mixer with a lens and a spiral antenna. Using a measurement setup with black body calibration sources and a beam splitter *in vacuo*, and an antireflection coated Si lens, we obtained a double sideband (DSB) receiver noise temperature ($T_{\mathrm{rec}}^{\mathrm{DSB}}$) of 1150 K, which is nine times $h\nu/2k$, where h is the Planck constant, ν the frequency, and k the Boltzmann constant. In addition, the measured far field beam patterns of the integrated lens antenna show nearly collimated beams from 2.5 to 5.3 THz that allow reliable measurement of $T_{\mathrm{rec}}^{\mathrm{DSB}}$ using the vacuum setup. Our experimental results in combination with an antenna-to-bolometer coupling simulation suggest that the HEB mixer can work well at least up to 6 THz, making it suitable for next generation of high-resolution spectroscopic space telescopes and, in particular, for the detection of the neutral atomic oxygen line at 4.7 THz. © *2010 American Institute of Physics*. [doi:10.1063/1.3503279]

I. INTRODUCTION

Superconducting hot electron bolometer (HEB) mixers are so far the most sensitive heterodyne detectors at frequencies above 1.5 THz. The HEB mixers based on NbN or NbTiN superconducting films have been successfully used to detect spectral lines up to 2 THz from ground based[1–3] and space telescopes.[4] The performance parameters, such as the low double sideband (DSB) receiver noise temperature ($T_{\mathrm{rec}}^{\mathrm{DSB}}$) of 1300 K at 4.3 THz,[5] an intermediate frequency (IF) gain bandwidth of 3 GHz and noise bandwidth of ~5 GHz,[6] low local oscillator (LO) power of 25–500 nW,[7] a spectroscopic Allan variance stability time of 3.5 s (Ref. 8) for a standard quasioptical NbN HEB mixer and a spectroscopic Allan variance stability time of 200 s for a balanced waveguide HEB mixer,[1] have been reported by different research groups. The HEB mixers become the detector of choice in the upper terahertz (THz) frequency range (3–6 THz) for high-resolution spectroscopic observations for astronomy.[9] One example is the fine-structure line of neutral atomic oxygen OI ($^3P_1-^3P_2$) at 4.7448 THz, which is a major coolant of dense interstellar medium and is a vital tool for probing the physical conditions of massive young stars.[10] The OI line has been recorded by a Schottky heterodyne receiver flying on the Kuiper Airborne Observatory.[11] However, the sensitivity of the receiver used was very poor and was 75 000 K at 4.7 THz. The sensitivity of a receiver, i.e., $T_{\mathrm{rec}}^{\mathrm{DSB}}$, is a crucial parameter that defines the minimal detectable line intensity and also the observation time.

Quasioptical radiation coupling scheme using a twin slot antenna in combination with a dielectric lens has been successfully applied to heterodyne mixers[4,12] up to 1.9 THz in the Herschel space observatory. We choose a spiral antenna in combination with a silicon lens in this work because it is broad band and can work at the high end of THz frequencies. The far field beam pattern of a quasioptical HEB mixer, governed by a lens/antenna combination and radiation frequency, is also an important performance parameter for a practical receiver. However, the beam pattern of a spiral antenna at 5 THz is not known, which motivates us to measure the beam. We notice that the beam patterns are crucial for correctly measuring $T_{\mathrm{rec}}^{\mathrm{DSB}}$ in our vacuum setup where hot/cold loads with a limited surface area are used.

The aim of this paper is to demonstrate experimentally the ultimate sensitivity of an NbN HEB mixer at the high end of the THz frequency range. Here, we use a similar HEB mixer and measurement setup as reported earlier for a measurement at 4.3 THz.[5] However, we extend the LO frequency to 5.25 THz. We report an extremely low $T_{\mathrm{rec}}^{\mathrm{DSB}}$ at 5.25 THz. In addition, the coupling efficiency between spiral antenna and bolometer is simulated. The far field beam patterns of the mixer were measured at several frequencies up to 5.25 THz.

II. HEB DEVICE AND MEASUREMENT SETUP

The HEB mixer used consists of a 2 μm wide, 0.2 μm long, and 5.5 nm thick NbN bridge on a highly resistive Si substrate. The NbN thin film was produced by a group at Moscow State Pedagogical University, Russia. The details of the NbN film can be found in Ref. 13. The bridge is con-

[a)]Electronic mail: wzhang@mail.pmo.ac.cn.
[b)]Electronic mail: j.r.gao@tudelft.nl.

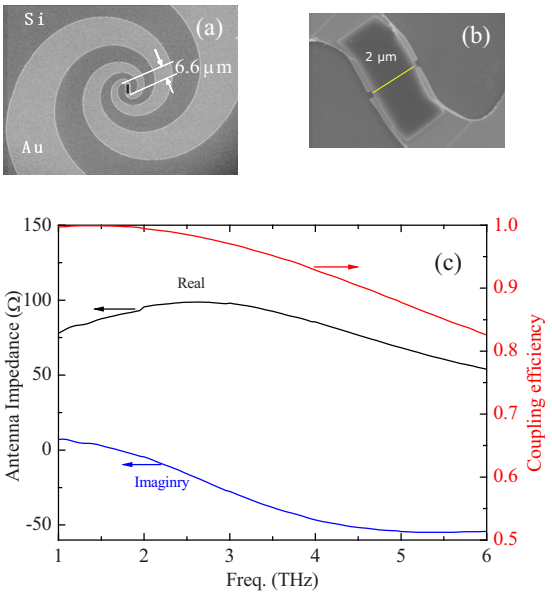

FIG. 1. (Color online) (a) SEM micrograph of a tight winding spiral antenna with an inner diameter of 6.6 μm; (b) SEM micrograph of the NbN bridge with a length of 0.2 μm and a width of 2 μm; and (c) simulated impedances of the spiral antenna vs frequency using HFSS and using the equivalent circuit (left axis) and calculated coupling efficiency between bolometer and antenna versus frequency (right axis).

nected to the antenna by Nb (10 nm)/Au (50 nm) superconducting bilayer contact pads.[14] Prior to deposition of the contact pads, Ar radio frequency (rf) sputter etching is applied to clean the surface of the NbN, eliminating contact resistance between NbN and contact pads. Such contact structures allow rf and dc power to be dissipated only in the NbN bridge, thus there is no rf loss and no additional noise contribution due to the contact interface. The antenna is an on-chip self-complementary spiral antenna that is made of a 170 nm thick Au layer. It has a tight winding design with an inner diameter of 6.6 μm close to the NbN bridge [Fig. 1(a)]. The HEB has a low-temperature normal-state resistance (R_N) of 83 Ω, a critical temperature of 9.3 K, and a critical current of 210 μA at 4.2 K.

We apply a similar vacuum measurement setup as described in Ref. 5 except for a different metal-mesh heat filter.[15] Furthermore, we do not use the band pass filter. The HEB chip is glued to the backside of Si elliptical lenses[16] without and with an antireflection coating, mounted in a mixer unit that is placed in a 4.2 K liquid helium cryostat. As calibration sources, a blackbody at 295 K is used as the hot load and another one at 77 K as the cold load. The two loads can be selected by rotating a mirror. The radiation from the hot/cold load is combined with that from the LO by a 3 μm Mylar beam splitter. Before reaching the HEB, the radiation passes through the heat filter at 4.2 K that blocks infrared radiation. There is no window on the cryostat and all these components are in the same vacuum unit.[17] Therefore, the radiation does not suffer from absorption due to water in the air and due to the window.

The LO is an optically pumped far infrared (FIR) ring gas laser, operated at a frequency of 5.2456 THz using CH_3OD gas, which is pumped by the 9R08 CO2 line. We choose this frequency because it provides enough power in the frequency range of interest. The LO power coupled to the mixer is regulated by rotating a wire grid in front of the gas laser.

The IF signal, resulting from the mixing of the LO and the hot/cold load signal, first passes through a bias-T, a circulator, and then a cryogenic low noise amplifier (Berkshire 1.3–1.7 GHz) operated at 4.2 K, followed by room-temperature amplifiers. This signal is filtered at 1.5 GHz within a band of 80 MHz. Between each two components in the IF chain, an attenuator is added to avoid standing waves. The entire IF chain has a gain of about 80 dB and a noise temperature of 7 K.

III. SIMULATION OF THE ANTENNA IMPEDANCE AND THE COUPLING

To predict the impedance of the antenna and further calculate the coupling efficiency of the radiation power from the antenna to the HEB at the upper THz frequencies, we model the antenna using a three-dimensional electromagnetic field simulator high frequency structure simulator (HFSS) (Ref. 18) based on finite element method. We assume that an rf signal is excited at the slit between two contact pads of the HEB, which is called a lumped port. The Si substrate with a refractive index $n_{Si}=3.42$ is set to be 20 μm thick, which is larger than 1/4 wavelength (λ) of the radiation in free space, required by HFSS. The electric conductivity of the 100 nm thick Au antenna layer is set to be 4.1×10^7 S/m. All the surfaces are taken as radiation boundaries to simulate the half-infinite space. To perform the simulation, the whole structure is first divided into many small elements, which are smaller than 0.05λ. For the regions where the electromagnetic field varies significantly it will be further automatically divided into even smaller elements to achieve accurate field and current distribution. The S parameters and Z parameters are then extracted from the electromagnetic field distribution. The input impedance ($Z_{antenna}=R_{antenna}+iX_{antenna}$) of the spiral antenna is Z_{11} of obtained Z matrix. Figure 1(c) shows the simulated $Z_{antenna}$ of the spiral antenna as a function of frequency between 1 and 6 THz. At lower frequencies the impedance is real and has a value close to 75 Ω as expected for an equiangular spiral antenna.[19] However, with increasing the frequency the reactive part appears and increases to -50 Ω at around 5 THz. The reactance can be explained by a parasitic effect that is due to the presence of a transition structure, namely the contact-pad structure between the HEB and the two arms of the spiral [see Fig. 1(b)], resulting in the electric and magnetic crowding effects.[20]

The coupling efficiency η can be calculated from S parameters

$$\eta = 1 - S_{11}^2. \quad (1)$$

The calculated η is also given in Fig. 1(c). We find that η is nearly 100% at the frequencies below 3 THz, while above this value it decreases gradually with increasing frequency. Even at the highest frequency of 6 THz, it is still more than 80%, suggesting that our particular spiral antenna with the tight winding design can work well up to at least 6 THz and even beyond this frequency.

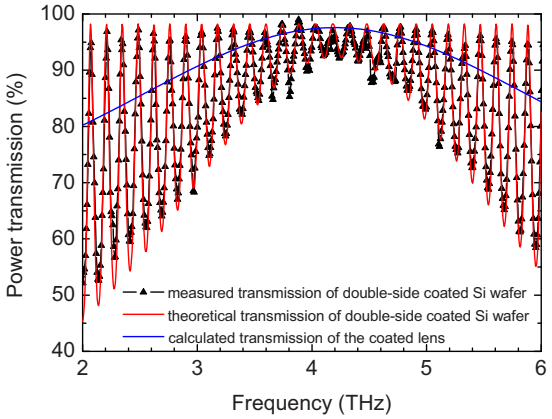

FIG. 2. (Color online) Measured and theoretical power transmission of a double-side polished Si wafer coated with a Parylene C layer on both sides. Calculated power transmission of coated lens (air+coating+Si) based on the obtained thickness and refractive index of Parylene C coating layer is also plotted vs frequency. The Si wafer and Parylene C coating layer are 2 mm and 10.9 μm thick, respectively.

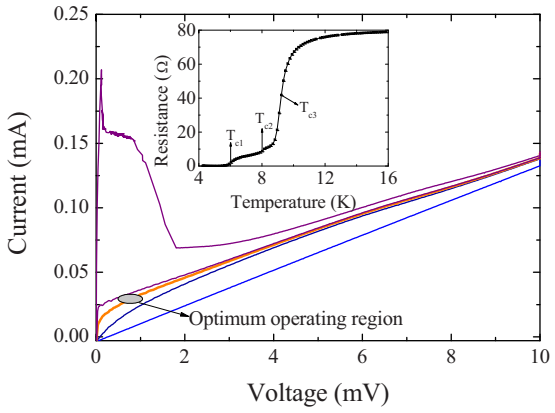

FIG. 3. (Color online) A set of current-voltage curves of the NbN HEB mixer at 4.2 K and at different LO power, where the optimum operating region is indicated. The inset shows the dc resistance versus temperature of a very similar HEB, which was measured in the low current limit.

IV. CHARACTERIZING AN ANTIREFLECTION COATING

It is known that when a Si lens is used to couple THz radiation from free space to an antenna, a considerable amount of optical loss is due to reflection because of the high refractive index of Si (n_{Si}). This loss can be minimized by coating an antireflection layer with a thickness of a quarter wavelength ($\lambda/4n_{AR}$) and with a refractive index $n_{AR}=n_{\mathrm{Si}}^{0.5}=1.85$. Parylene C is a known coating material[21] since it has a refractive index (n_{PC}) of 1.65, which is close to the optimum value.

To measure the ultimate $T_{\mathrm{rec}}^{\mathrm{DSB}}$ at 5.25 THz, we apply an existing Si lens coated with Parylene C. The coating layer has a thickness of 10.9 μm and was originally designed for 4.3 THz.[5] To find its transmission at 5.25 THz, we prepared a double-side polished Si wafer coated with a Parylene C layer of the same thickness (10.9 μm) on both sides and measured the power transmission as a function of frequency with a Fourier transform spectrometer. The measured result is shown in Fig. 2. The measured data are fitted by a theoretical model based on multiple reflection and transmission for plane-parallel dielectrics[22] to find the thickness d_{PC}, refractive index n_{PC} and absorption coefficient α_{PC} of Parylene C. Based on the obtained parameters ($d_{PC}=10.93$ μm, $n_{PC}=1.634$, and $\alpha_{PC}=7.17/\mathrm{cm}$), the transmission for a vacuum/Parylene C/Si interface as a function of frequency is calculated and also depicted in Fig. 2. At 5.25 THz the transmission reaches 92%, which is 22% higher compared to that of a vacuum/Si interface. Based on this result, we expect this amount of reduction in the reflection loss at 5.25 THz when we apply this antireflection coated lens. As a result, we should expect roughly a reduction in the receiver noise temperature by 22%. We also find that at the designed frequency (4.3 THz), the transmission reaches its maximum of 97%.

V. EXPERIMENTAL RESULTS

A. R-T curve and pumped *I-V* curves of the HEB mixer

The resistance of a similar HEB from the same fabrication run has been measured as a function of temperature. The result is shown in the inset of Fig. 3. It is featured by three superconducting transitions. The lowest transition T_{c1} of 6 K is associated with the Au/Nb/NbN contact structures; the middle transition T_{c2} of 8 K is associated with the NbN under Au (thick) antenna layer; and the highest transition T_{c3} of 9.3 K is due to the NbN bridge. The resistance above T_{c3} is about 83 Ω making a good impedance match possible with the spiral antenna. It is important to mention that in our case when the HEB is operated at the optimal biasing point, the contacts are in the superconducting state. More discussions of the superconducting transitions in such structures can be found elsewhere.[14]

A typical set of *I-V* curves of the HEB with different LO power levels at 5.25 THz, recorded at 4 K, is shown in Fig. 3. With increasing LO power level, the superconductivity of the NbN bridge becomes gradually suppressed, showing a transition from the superconducting state to the normal one. The measured curves can be explained by a nonuniform distribution model for a HEB.[23] The optimum operating region, where the lowest $T_{\mathrm{rec}}^{\mathrm{DSB}}$ can be obtained, is indicated in the *I-V* plot. This region is centered at a bias voltage of 0.6 mV and a current of 34 μA. The optimum LO power in the HEB is about 150 nW, obtained by the isothermal technique and making use of the *I-V* curves at the high bias voltage region.[24,25] The LO power required for a HEB is known to be proportional to its area and its critical temperature (in our case T_{c3}).[7]

B. Receiver noise temperature at 5.25 THz

We start with a measurement in which the HEB is mounted on the uncoated Si lens and $T_{\mathrm{rec}}^{\mathrm{DSB}}$ is characterized in a conventional way. We measured the output power of the receiver, $P_{\mathrm{out,hot}}$ and $P_{\mathrm{out,cold}}$, responding to the hot and cold

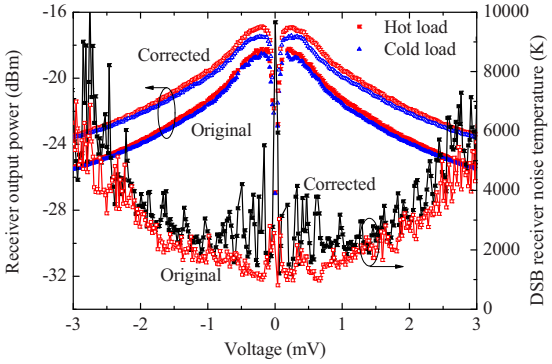

FIG. 4. (Color online) Measured receiver output power (left axis) responding to the hot (square) and cold load (triangle) at optimum LO power as a function of bias voltage. One set of data (solid square and triangle) are measured with fixed LO power level and another set (open square and triangle) by adjusting LO power such that the current is the same for hot and cold loads (2 dB positive offset is introduced in the plot for clarity). The resulted DSB receiver noise temperatures are also plotted vs bias voltage (right axis).

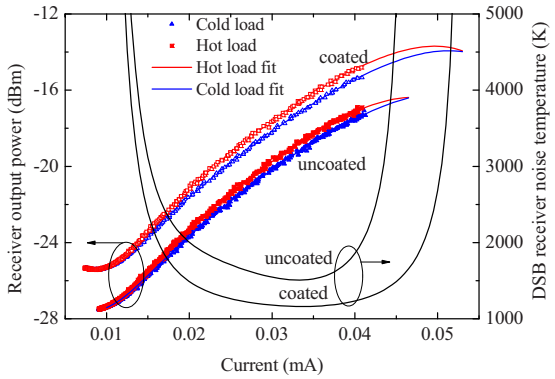

FIG. 5. (Color online) Measured receiver output powers at the optimum bias voltage of 0.6 mV (dots) and the polynomial fit (lines) responding to the hot and cold load as a function of bias current of the HEB, which is varied by changing the LO power (left axis). One set of data are measured using uncoated lens and another set of data (2 dB positive offset for clarity) are measured using a coated lens. The resulted DSB receiver noise temperature curves are also shown as a function of bias current of the HEB (right axis).

load as a function of bias voltage under a constant, but optimum LO power. The results are plotted in Fig. 4. $T_{\mathrm{rec}}^{\mathrm{DSB}}$ is obtained by the Y-factor method and using the equivalent temperatures for the blackbody at 295 and 77 K according to the Callen–Welton definition.[26] $T_{\mathrm{rec}}^{\mathrm{DSB}}$ as a function of bias voltage is also plotted in Fig. 4. The lowest $T_{\mathrm{rec}}^{\mathrm{DSB}}$ (black dot line) is roughly 2000 ± 500 K. The uncertainties are mainly caused by the LO power fluctuations and drift. As to be shown in Sec. V C, the stability of the output power of our gas laser is on the order of 2%, which leads to about 4% instability in the Y-factor and about 25% fluctuations in the measured $T_{\mathrm{rec}}^{\mathrm{DSB}}$.

It has been well established that a HEB with a wideband antenna and low LO power requirement can suffer from the direct detection effect due to broadband blackbody radiation.[27] In our case this effect becomes significant due to a combination of the lossless hot/cold blackbody radiation *in vacuo* and the wide rf bandwidth of the antenna. An additional demonstration of the direct detection effect in this particular experiment will be given in Sec. V C. As a result, a measured $T_{\mathrm{rec}}^{\mathrm{DSB}}$ is usually higher than it should be.[27] This effect can be corrected out by adjusting LO power such that the dc current of the HEB is the same responding to the hot and cold loads. For comparison, the receiver output power data after adjusting LO power are also shown in Fig. 4. For clarity a 2 dB positive offset in the vertical direction is introduced in the plot. The measured lowest $T_{\mathrm{rec}}^{\mathrm{DSB}}$ becomes 1500 ± 300 K, which is on average 25% lower than what measured previously.

By applying a different characterization method[5] we can directly measure $T_{\mathrm{rec}}^{\mathrm{DSB}}$, without suffering from both the direct detection and the instability of the gas laser. At the bias voltage of 0.6 mV we measure the receiver output power as a function of bias current, which is the result of varying LO power. Two such data sets are recorded, $P_{\mathrm{out,hot}}(I)$ responding to the hot load and $P_{\mathrm{out,cold}}(I)$ to the cold load. The Y factor can be obtained by $Y(I)=P_{\mathrm{out,hot}}(I)/P_{\mathrm{out,cold}}(I)$ at the same current using the fitted polynomial curves to the $P_{\mathrm{out,hot}}(I)$ and $P_{\mathrm{out,cold}}(I)$ data points. The calculated $T_{\mathrm{rec}}^{\mathrm{DSB}}$ as a function of bias current is plotted in Fig. 5 and shows a broad minimum at a bias current of around 34 μA and the lowest value of 1550 ± 50 K. This is in good agreement with the value measured in the conventional way but after correcting the direct detection effect. As discussed in Ref. 5, a clear advantage of this method is that the $T_{\mathrm{rec}}^{\mathrm{DSB}}$ can be determined precisely and is independent of LO power instability. This is because LO power is used as a variable. Any data point at any LO power is a useful contribution to the P_{out}-I curve. In contrast to the standard manner, where the LO power is required to be fixed, here, it is used as a variable. Another advantage with this method is that the Y-factor and thus the $T_{\mathrm{rec}}^{\mathrm{DSB}}$ are not influenced by the direct detection effect because $P_{\mathrm{out,hot}}$ and $P_{\mathrm{out,cold}}$ are taken at exactly the same bias point. We also measured the mixer conversion loss using a method by Ref. 28 and find it to be about 8.8 dB.

Now we measure $T_{\mathrm{rec}}^{\mathrm{DSB}}$ of the same HEB but mounted on the coated Si lens. Again, we measure at the optimum bias voltage of 0.6 mV. The data are added in Fig. 5. For clarity, the receiver output power data as a function of current, responding to hot/cold loads, are offset positively by 2 dB. The lowest $T_{\mathrm{rec}}^{\mathrm{DSB}}$ obtained is 1150 ± 40 K, which is about 26% lower than the value (1550 K) measured previously using the uncoated lens. This difference is consistent reasonably with what is expected from using the antireflection coating layer (22%), as described in Sec. IV of this paper. Table I summarizes the optical loss at 5.25 THz for both cases.

To make a comparison with the measured $T_{\mathrm{rec}}^{\mathrm{DSB}}$ at 5.25 THz reported previously by other group,[29] we also performed a noise measurement in a standard measurement setup in air. In this case, we have the optical loss of 6.8 dB in total, contributed not only by the beam splitter, the metal-mesh heat filter, and uncoated Si lens (as given in Table I), but also by a window, two Zitex heat filters, and air. We measured a $T_{\mathrm{rec}}^{\mathrm{DSB}}$ of 3800 K at 5.25 THz, which is about a factor of 2 better than the one reported in Ref. 29, where the total optical loss is 5.6 dB. We attribute the improvement to the fact that we applied an NbN HEB mixer with cleaned and superconducting contact structures[30] and optimized design of the antenna structure. Although our measurement method

TABLE I. Summary of DSB receiver noise temperature data at 5.25 THz, measured at four different cases with the same HEB mixer: (1) the air setup: a 3 μm Mylar beam splitter, a metal-mesh heat filter, two Zitex heat filters, a window, air, and an uncoated Si lens; (2) the vacuum setup: a 3 μm Mylar beam splitter, a metal-mesh heat filter, two Zitex heat filters, and an uncoated Si lens; (3) the vacuum setup (no Zitex): the same as (2) but removing the two Zitex heat filters; and (4) the vacuum setup (coated lens): the same as (3) but replacing with a coated Si lens. All the relevant parameters are also listed: optical loss of the 3 μm Mylar beam splitter at 300 K (L_{BS}, calculated), the metal-mesh heat filter at 4 K (L_{filter}, measured), the two Zitex heat filters at 4 K [L_{Zitex}(dB), measured], the window at 300 K [L_{window}(dB), measured], the coated and uncoated Si lens at 4 K [L_{lens}(dB), reflection loss calculated; absorption loss is negligible based on our measurements on a Si wafer from the same material as used for our Si lens], and DSB receiver noise temperature [T_{rec}^{DSB}(K), measured].

	L_{BS} (dB)	L_{filter} (dB)	L_{Zitex} (dB)	L_{window} (dB)	L_{air} (dB)	L_{lens} (dB)	T_{rec}^{DSB} (K)
Air setup	0.71	0.81	2.1	1.2	0.5	1.5	3800
Vacuum setup	0.71	0.81	2.1			1.5	2600
Vacuum setup (no Zitex)	0.71	0.81				1.5	1550
Vacuum setup(coated lens)	0.71	0.81				0.36	1150

avoids the influence of the direct detection, the latter plays a negligible role in this specific measurement because of the relatively high optical loss.

The T_{rec}^{DSB} of 1150 K represents the highest heterodyne sensitivity ever measured at 5.25 THz. Several factors are considered to be crucial for this result. First, our device has contacts between HEB and antenna which do not have contact resistance[30,31] As a result, no radiation loss and no additional noise contribution due to the contacts are expected. Second, our spiral antenna design allows a high radiation coupling efficiency even up to 6 THz. Third, the use of the measurement setup *in vacuo* and the thin beam splitter reduces the optical loss to the minimum. Fourth, T_{rec}^{DSB} is not influenced by the direct detection effect because of the application of the characterization method as in Ref. 5. As shown in Ref. 32, fundamentally our HEB mixer has the same classical output noise level (35 K due to Johnson noise and thermal fluctuation noise) at any LO frequency between 1.5–5.3 THz and has a similar mixer conversion loss. The only factors that can affect T_{rec}^{DSB} at 5.25 THz are the radiation coupling efficiency between free space and the HEB and the quantum noise. It is interesting to notice that at this frequency the quantum noise plays a significant role and contributes roughly 50% to the receiver noise temperature.[32]

C. Direct detection

Figure 6 shows the measured receiver output power, together with the dc current of the HEB, as a function of time over a period of 150 s, during which the hot and cold loads are manually switched after roughly every 5 s. The HEB in this case is mounted on the coated lens. The bias voltage is fixed at 0.8 mV and the LO power set at the optimal value. The periodic jumps of $\leq$0.3 dB in the receiver output power between the hot and cold load should reflect directly how large the Y-factor is. However, the actual value is affected by the direct detection effect.[27] This effect is demonstrated by the observed jumps in the current switching between hot and cold load, which is about 1.2 μA in amplitude. We attribute this change in the current to the increase in the noise temperature by $\sim$25% due to the direct detection effect as discussed previously. In principle, the direct detection effect can be minimized or eliminated by reducing the blackbody radiation power, for example, by adding a narrow band pass filter in front of the mixer.[5,25]

The absolute value of the bias current of the HEB when it is optimally pumped by LO varies less than 2% during the measurement period in Fig. 6, which indicates that our gas laser is stable enough to measure the Y-factor under a fixed LO power in a conventional way. However, the variations can cause considerable fluctuations in T_{rec}^{DSB}, as shown in Fig. 4 and discussed in Sec. V B.

D. Beam patterns of the lens/antenna

The far field beam patterns of the same HEB mixer on the uncoated Si lens are measured at several frequencies from 2.5 to 5.25 THz using a computer controlled setup as described previously.[33] We apply the same gas laser as a signal source to measure the beams of the mixer. A FIR gas laser is known to have a narrow, collimated beam. The HEB cryostat is placed on a rotation/tilt table in the far field of the gas laser, which has a linearly polarized electrical field in the vertical direction. The center of the spiral antenna is located in the center of the rotation. The measured beam pattern of lens/antenna combination is therefore expected to be independent of beam pattern of the signal source.

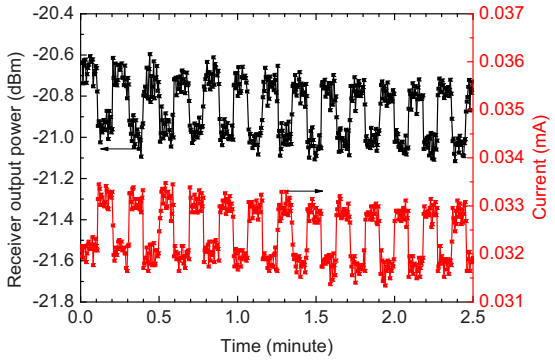

FIG. 6. (Color online) Measured receiver output power (left axis) and bias current of the HEB (right axis) as functions of time over a period of 150 s, during which the hot and cold loads are manually switched after roughly each 5 s.

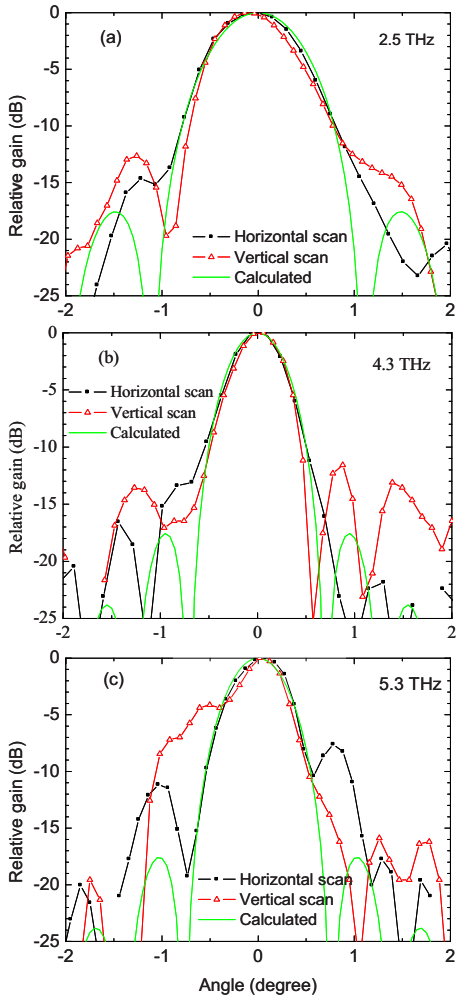

FIG. 7. (Color online) Measured and simulated far field beam patterns of the HEB mixer on the uncoated Si lens, which are the same as used for the sensitivity measurements at 2.5 THz (a), 4.3 THz (b), and 5.25 THz (c). The scans are made for both horizontal and vertical directions. The horizontal scan is indicated by black solid square+line; while the vertical scan by red hollow triangle+line.

The HEB is heated to a temperature that is slightly below the superconducting transition temperature of the NbN bridge T_{c3}. It is voltage biased and the current changes due to the modulated incident power are measured as a function of the angle of rotation/tilt by a lock-in amplifier. The tilt movement is referred to as vertical scan and the rotation as horizontal scan. The dynamic range of the setup is about 20 dB. The antenna is positioned in such a way that the direction along the NbN bridge width is about 30° counterclockwise from the vertical direction of the setup.

Figure 7 shows the beam patterns, measured in both horizontal and vertical directions of the integrated lens/antenna at 2.5, 4.3, and 5.25 THz. The main lobes are similar in horizontal and vertical scans, which indicate that our beam patterns are almost rotationally symmetric. At the measured frequencies the beam pattern of the integrated lens antenna is diffraction limited,[34] and can be simulated according to the expression $[2J_1(\upsilon)/\upsilon]^2$, where $\upsilon=[\pi \tan(\theta)d]/\lambda$, θ is the angle, and J_1 is the Bessel function of the first kind, and d the effective diffracting aperture, which is varied to yield the best fit to the main lobe of the measured beam pattern. The full width at half maximum at 5.25 THz is 0.65°, which is similar to 0.6° at 4.3 THz, but smaller than 0.9° at 2.5 THz. Such small angles suggest that the main beams at these frequencies are nearly parallel or almost collimated. The main beam becomes narrower from 2.5 to 4.3 THz due to wavelength, while it is almost the same between 4.3 and 5.25 THz, indicating the effective aperture at 5.25 THz is smaller. The difference in the side lobes is likely due to the combination of antenna misalignment to the Si lens (within an accuracy of 5 μm) and the measurement setup. Especially at 5.25 THz the beam profile in vertical scan has a large shoulder [see Fig. 7(c)], the reason for which is still unclear. The first side lobes at 2.5 THz, 4.3 THz, and 5.25 THz occur at −13 dB, −11 dB, and −7 dB, respectively, increasing with increasing frequency.[34] The physical reasons for this are the internal reflection and surface roughness.[35,36]

The nearly collimated (main) beam at 5.25 THz is confirmed by a separated measurement. Taking the beam width (radius) at the mixer to be the radius of the Si lens (5 mm),[37] we should expect a beam with a diameter of 16 mm at the position of the cold load, which is 290 mm away from the HEB and is the longest distance in the optical path in our vacuum setup. By varying the effective diameter of hot/cold loads at the same distance (290 mm), which in this case are not *in vacuo*, we found that $T_{\mathrm{rec}}^{\mathrm{DSB}}$ is independent of the size of the hot/cold loads if it is increased from 30 mm to, e.g., 100 mm. This experiment suggests that the beam diameter in this case should be smaller than 30 mm. We expect it to be around 16 mm. However, we did not perform a direct measurement. The nearly collimated beams are also the case for other frequencies down to at least 2.5 THz. Such beams are crucial for correctly measuring $T_{\mathrm{rec}}^{\mathrm{DSB}}$ using the vacuum setup.

VI. SUMMARY

We have demonstrated a highly sensitive spiral antenna coupled NbN HEB mixer at 5.25 THz. We measured the lowest $T_{\mathrm{rec}}^{\mathrm{DSB}}$ of 1150 K at 5.25 THz. Based on this and the newly measured $T_{\mathrm{rec}}^{\mathrm{DSB}}$ at 4.3 THz (860 K), we expect a $T_{\mathrm{rec}}^{\mathrm{DSB}}$ of 1000 K at 4.7 THz. It is worthwhile to note that this sensitivity at 4.7 THz is about 75 times better than a Schottky diode mixer at the same frequency.[11] We also present the far field beam pattern of the mixer at 5.25 THz, which shows a beam with small divergence and the side lobe of −7 dB. With further improvement of the beam pattern, such a mixer together with recently developed THz quantum cascade lasers (QCL) as LO should allow the construction of new receivers[38,39] for detecting OI line at 4.7 THz for future airborne and space-borne telescopes. Much progress has been made on THz QCLs with regard to the operating frequency, temperature, output power, phase locking,[40–42] and heterodyne high-resolution spectroscopic measurement with a gas cell,[43] making them ready for applications.

ACKNOWLEDGMENTS

We acknowledge E. L. Kollberg and K. S. Yngvesson for very useful discussions, L. de Jong, W. M. Laauwen, and J. N. Hovenier for their technical support, and W. Horinga for the FTS transmission measurement. The work was supported

by the NSFC under Grant Nos. 10803021 and 10621303, by China Exchange Programme executed by KNAW and CAS, and by the AMSTAR+project of RadioNet under FP7 and NWO.

[1]D. Meledin, A. Pavolotsky, V. Desmaris, I. Lapkin, C. Risacher, V. Perez, D. Henke, O. Nystrom, E. Sundin, D. Dochev, M. Pantaleev, M. Fredrixon, M. Strandberg, B. Voronov, G. Goltsman, and V. Belitsky, IEEE Trans. Microwave Theory Tech. **57**, 89 (2009).
[2]J. Kawamura, T. R. Hunter, C. E. Tong, R. Blundell, D. C. Papa, F. Patt, W. Peters, T. Wilson, C. Henkel, G. Gol'tsman, and E. Gershenzon, Astron. Astrophys. **394**, 271 (2002).
[3]M. C. Wiedner, G. Wieching, F. Bielau, K. Rettenbacher, N. H. Volgenau, M. Emprechtinger, U. U. Graf, C. E. Honingh, K. Jacobs, B. Vowinkel, K. M. Menten, L.-A. Nyman, R. Gusten, S. Philipp, D. Rabanus, J. Stutzki, and F. Wyrowski, Astron. Astrophys. **454**, L33 (2006).
[4]S. Cherednichenko, V. Drakinskiy, T. Berg, P. Khosropanah, and E. Kollberg, Rev. Sci. Instrum. **79**, 034501 (2008).
[5]P. Khosropanah, J. R. Gao, W. M. Laauwen, M. Hajenius, and T. M. Klapwijk, Appl. Phys. Lett. **91**, 221111 (2007).
[6]S. Cherednichenko, P. Khosropanah, E. Kollberg, M. Kroug, and H. Merkel, Physica C **372–376**, 407 (2002).
[7]J. J. A. Baselmans, M. Hajenius, J. R. Gao, A. Baryshev, J. Kooi, T. M. Klapwijk, B. Voronov, P. de Korte, and G. Gol'tsman, IEEE Trans. Appl. Supercond. **15**, 484 (2005).
[8]J. W. Kooi, J. J. A. Baselmans, A. Baryshev, R. Schieder, M. Hajenius, J. R. Gao, T. M. Klapwijk, B. Voronov, and G. Gol'tsman, J. Appl. Phys. **100**, 064904 (2006).
[9]http://www.sofia.usra.edu/
[10]R. Gusten, P. Hartogh, H.-W. Hubers, U. Graf, K. Jacobs, H. P. Poser, F. Schafer, R. Schieder, R. Stark, J. Stutzki, P. Van der Wal, and A. Wunsch, Proc. SPIE **4014**, 23 (2000).
[11]R. T. Boreiko and A. L. Betz, Astrophys. J. **464**, L83 (1996).
[12]A. Karpov, D. Miller, F. Rice, J. A. Stern, B. Bumble, H. G. LeDuc, and J. Zmuidzinas, Proc. SPIE **6275**, 62751U (2006).
[13]J. R. Gao, M. Hajenius, F. D. Tichelaar, T. M. Klapwijk, B. Voronov, E. Grishin, G. Gol'tsman, C. A. Zorman, and M. Mehregany, Appl. Phys. Lett. **91**, 062504 (2007).
[14]T. Aggarwal, P. Khosropanah, W. Zhang, F. D. Tichelaar, J. R. Gao, and T. M. Klapwijk, Proceedings of 19th International Symposium on Space Terahertz Technology, Groningen, The Netherlands, 28–30 April 2008 (unpublished), pp. 398–402.
[15]The metal-mesh heat filter has an upper cutoff frequency of 6 THz and 0.8 dB loss at 5.25 THz and is produced by QMC Ltd.
[16]HEB chip is placed on the backside of an elliptical Si lens, which is governed by the equation of $(x/a)^2+(y/b)^2=1$ with a major radii b =5.228 mm and a minor radii a=5 mm. The extension from geometric center of the elliptical lens is 1.229 mm and the Si substrate of the HEB chip is 340 μm thick.
[17]The vacuum unit consists of a beam splitter (which is changeable), a hot and cold load, and a rotating mirror. The beam splitter (3 μm Mylar) with a diameter of 22 mm is 35 mm away from the cryostat (the position of the window if it is there). The hot and cold loads with a diameter of 30 mm are 140 mm and 230 mm, respectively, away from the cryostat.
[18]3D full-wave electromagnetic field simulation, see http://ansoft.com/products/hf/HFSS/
[19]J. D. Dyson, IRE Trans. Antennas Propag. **7**, 181 (1959).
[20]P. Focardi, A. Neto, and W. McGrath, IEEE Trans. Microwave Theory Tech. **50**, 2374 (2002).
[21]H.-W. Hübers, J. Schubert, A. Krabbe, M. Birk, G. Wagner, A. Semenov, G. Goltsman, B. Voronov, and E. Gershenzon, Infrared Phys. Technol. **42**, 41 (2001).
[22]M. Born and E. Wolf, *Principles of Optics*, 6th ed. (Pergamon, New York, 1980).
[23]R. Barends, M. Hajenius, J. R. Gao, and T. M. Klapwijk, Appl. Phys. Lett. **87**, 263506 (2005).
[24]H. Ekstrom, B. Karasik, E. Kollberg, and S. Yngvesson, IEEE Trans. Microwave Theory Tech. **43**, 938 (1995).
[25]M. Hajenius, J. J. A. Baselmans, A. Baryshev, J. R. Gao, T. M. Klapwijk, J. W. Kooi, W. Jellema, and Z. Q. Yang, J. Appl. Phys. **100**, 074507 (2006).
[26]A. R. Kerr, IEEE Trans. Microwave Theory Tech. **47**, 325 (1999).
[27]J. J. A. Baselmans, A. Baryshev, S. F. Reker, M. Hajenius, J. R. Gao, T. M. Klapwijk, B. Voronov, and G. Gol'tsman, J. Appl. Phys. **100**, 084510 (2006).
[28]S. Cherednichenko, M. Kroug, H. Merkel, P. Khosropanah, A. Adam, E. Kollberg, D. Loudkov, G. Gol'tsman, B. Voronov, H. Richter, and H.-W. Huebers, Physica C **372–376**, 427 (2002).
[29]A. D. Semenov, H.-W. Hübers, J. Schubert, G. N. Gol'tsman, A. I. Elantiev, B. M. Voronov, and E. M. Gershenzon, J. Appl. Phys. **88**, 6758 (2000).
[30]M. Hajenius, J. J. A. Baselmans, J. R. Gao, T. M. Klapwijk, P. A. J. de Korte, B. Voronov, and G. Gol'tsman, Supercond. Sci. Technol. **17**, S224 (2004).
[31]T. M. Klapwijk, R. Barends, J. R. Gao, M. Hajenius, and J. J. A. Baselmans, Proc. SPIE **5498**, 129 (2004).
[32]W. Zhang, P. Khosropanah, J. R. Gao, E. L. Kollberg, K. S. Yngvesson, T. Bansal1, R. Barends, and T. M. Klapwijk, Appl. Phys. Lett. **96**, 111113 (2010).
[33]P. Yagoubov, W. J. Vreeling, and P. de Korte, Proceedings of 12th International Symposium on Space Terahertz Technology, San Diego, California, 14–16 February 2001 (unpublished), pp. 193–199.
[34]H.-W. Hüber, A. D. Semenov, H. Richter, J. Schubert, S. Hadjiloucas, J. W. Bowen, G. N. Goltsman, B. M. Voronov, and E. M. Gershenzon, Proceedings of 12th International Symposium on Space Terahertz Technology, San Diego, California, 14–16 February 2001 (unpublished), pp. 286–296.
[35]M. J. M. van der Vorst, P. J. I. de Maagt, A. Netto, A. L. Reynolds, R. M. Heeres, W. Luinge, and M. H. A. J. Herben, IEEE Trans. Microwave Theory Tech. **49**, 1118 (2001).
[36]A. D. Semenov, H. Richterm, H.-W. Hübers, B. Gunther, A. Smirnov, K. S. Il'in, M. Siegel, and J. P. Karamarkovic, IEEE Trans. Microwave Theory Tech. **55**, 239 (2007).
[37]D. F. Filipovic, S. S. Gearhart, and G. M. Rebeiz, IEEE Trans. Microwave Theory Tech. **41**, 1738 (1993).
[38]J. R. Gao, J. N. Hovenier, Z. Q. Yang, J. J. A. Baselmans, A. Baryshev, M. Hajenius, T. M. Klapwijk, A. J. L. Adam, T. O. Klaassen, B. S. Williams, S. Kumar, Q. Hu, and J. L. Reno, Appl. Phys. Lett. **86**, 244104 (2005).
[39]H.-W. Hübers, S. G. Pavlov, A. D. Semenov, R. Köhler, L. Mahler, A. Tredicucci, H. E. Beere, D. A. Ritchie, and E. H. Linfield, Opt. Express **13**, 5890 (2005).
[40]D. Rabanus, U. U. Graf, M. Philipp, O. Ricken, J. Stutzki, B. Vowinkel, M. C. Wiedner, C. Walther, M. Fischer, and J. Faist, Opt. Express **17**, 1159 (2009).
[41]P. Khosropanah, A. Baryshev, W. Zhang, W. Jellema, J. N. Hovenier, J. R. Gao, T. M. Klapwijk, D. G. Paveliev, B. S. Williams, S. Kumar, Q. Hu, J. L. Reno, B. Klein, and J. L. Hesler, Opt. Lett. **34**, 2958 (2009).
[42]S. Barbieri, P. Gellie, G. Santarelli, L. Ding, W. Maineult, C. Sirtori, R. Colombelli, H. Beere, and D. Ritchie, Nature Photonics **4**, 636 (2010).
[43]Y. Ren, J. N. Hovenier, R. Higgins, J. R. Gao, T. M. Klapwijk, S. C. Shi, A. Bell, B. Klein, B. S. Williams, S. Kumar, Q. Hu, and J. L. Reno, "Terahertz heterodyne spectrometer using a quantum cascade laser," Appl. Phys. Lett. (in press).